Published in final edited form as:
Neuroimage. 2010 November 1; 53(2): 653–663. doi:10.1016/j.neuroimage.2010.06.062.

Engagement of large-scale networks is related to individual differences in inhibitory control

Eliza Congdon[*,a,b], **Jeanette A. Mumford**[c], **Jessica R. Cohen**[d], **Adriana Galvan**[a], **Adam R. Aron**[e], **Gui Xue**[f], **Eric Miller**[a], and **Russell A. Poldrack**[a,c,g]

[a]Department of Psychology, University of California Los Angeles, Los Angeles, CA, USA

[b]Center for Neurobehavioral Genetics, University of California Los Angeles, Los Angeles, CA, USA

[c]Department of Psychology, University of Texas at Austin, Austin, TX, USA

[d]Department of Psychology, University of California Berkeley, Berkeley, CA, USA

[e]Department of Psychology, University of California San Diego, San Diego, CA, USA

[f]Department of Psychology, University of Southern California, Los Angeles, CA, USA

[g]Department of Neurobiology, University of Texas at Austin, Austin, TX, USA

Abstract

Understanding which brain regions regulate the execution, and suppression, of goal-directed behavior has implications for a number of areas of research. In particular, understanding which brain regions engaged during tasks requiring the execution and inhibition of a motor response provides insight into the mechanisms underlying individual differences in response inhibition ability. However, neuroimaging studies examing the relation between activation and stopping have been inconsistent regarding the direction of the relationship, and also regarding the anatomical location of regions that correlate with behavior. These limitations likely arise from the relatively low power of vox-elwise correlations with small sample sizes. Here, we pooled data over five separate fMRI studies of the Stop-signal task in order to obtain a sufficiently large sample size to robustly detect brain/behavior correlations. In addition, rather than performing mass univariate correlation analysis across all voxels, we increased statistical power by reducing the dimensionality of the data set using independent components analysis and then examined correlations between behavior and the resulting component scores. We found that components reflecting activity in regions thought to be involved in stopping were associated with better stopping ability, while activity in a default-mode network was associated with poorer stopping ability across individuals. These results clearly show a relationship between individual differences in stopping ability in specific activated networks, including regions known to be critical for the behavior. The results also highlight the usefulness of using dimensionality reduction to increase the power to detect brain/behavior correlations in individual differences research.

[*]Corresponding Author: Eliza Congdon, Ph.D., Department of Psychology and Center for Neurobehavioral Genetics, Franz Hall, Box 951563, Los Angeles, CA 90095-1563, phone: 310-794-1139, fax: 310-206-5895, econgdon@ucla.edu.

Keywords

response inhibition; Stop-signal; independent components analysis; fMRI; individual differences

Introduction

Understanding the relationship between trait or performance measures and task-induced neural activation represents a line of research that offers great potential for elucidating mechanisms of individual differences in cognitive function, as well as cognitive dysfunction. The role of individual differences in response inhibition is a particularly attractive area as it has widespread implications for executive control. However, this line of research is limited by the need to include a sufficiently large sample size in order to capture variability and to have adequate power for analysis. This is amplified in fMRI studies of individual differences that have used mass univariate (voxelwise) analyses, which are plagued by multiple comparisons problems.

In order to achieve sufficient power, and to fully characterize the pattern of individual differences in neural activation underlying response inhibition, we combined data from five separate fMRI studies that included scanning during performance of the Stop-signal task, a widely used measure of response inhibition. Although we conducted whole-brain correlation analyses for comparison, we also conducted probabilistic independent components analysis (ICA) as a form of data dimensionality reduction. This approach allowed us to correlate behavior with loading coefficients for each subject on components resulting from ICA, which reflect spatially independent networks of activation. Our results demonstrate that this approach to dimensionality reduction 1) greatly reduces the multiple comparison issues common to this line of research; 2) substantially improves power for individual differences research; and 3) teases apart the role of functionally integrated networks underlying individual differences in response inhibition.

Response inhibition is the ability to suppress a prepotent or habitual response, including both motor actions and higher-order responses (such as thoughts, memories, or emotions) and is therefore critical to the ability to stop or suppress rapid, automatic behaviors in response to goals or environmental contingencies (Cools, 2008; Jentsch and Taylor, 1999; Nigg et al., 2005). The clinical significance of response inhibition is supported by a wide range of studies demonstrating impaired inhibition associated with disorders including Attention Deficit/Hyperactivity Disorder (ADHD) (Lijffijt et al., 2005; Oosterlaan et al., 1998; Schachar et al., 2005; Schachar and Logan, 1990), substance abuse (Ersche et al., 2008; Fillmore and Rush, 2002, 2006; Monterosso et al., 2005), Conduct disorder (CD) and comorbid CD/ADHD (Oosterlaan et al., 1998). For example, as compared to healthy controls, substance abusers show poorer ability to inhibit behavioral responses on a Stop-signal task, but unimpaired ability to execute responses on Go trials (Fillmore and Rush, 2002; Monterosso et al., 2005). Evidence that the impairment of drug abusing samples in performance of these tasks is specific to the inhibition, and not the execution, of a response underscores the clinical significance of mechanisms underlying response inhibition. In addition, there is evidence that response inhibition is correlated with measures of self-reported impulsivity in the healthy population (Avila and Parcet, 2001; Logan et al., 1997) (but see Enticott et al. (2006)).

Laboratory measures of response inhibition, such as the Go/NoGo and Stop-signal paradigms, require participants to respond on a set of relatively frequent trials (Go trials), but to inhibit responding to a separate set of infrequent (Stop trials) (Chambers et al., 2009; Verbruggen and Logan, 2009). In addition, response inhibition is thought to be involved across a number of other paradigms, including response interference, switching, and reversal learning tasks, and the common factor linking these tasks appears to be the need to maintain a goal in the face of

strongly activated, but inappropriate, representations or distracting stimuli (Friedman and Miyake, 2004). An advantage of the Stop-signal task is the use of an adaptive procedure to determine the delay at which the stop signal must be presented in order to result in successful stopping on 50% of trials, which makes greater demands on a participants inhibitory control. The Stop-signal task is based on a horse-race model, which assumes that independent go and stop processes race against one another to determine whether a response is executed or inhibited (Logan and Cowan, 1984; Logan, 1994) (though the independence assumption can be relaxed (Boucher et al., 2007)). This model allows for the estimation of a measure called the stop-signal reaction time (SSRT), an individualized measure of a participant's inhibitory ability that controls for difficulty level. It has been shown to distinguish individuals with impaired inhibitory control from healthy controls (Lijffijt et al., 2005; Rucklidge and Tannock, 2002). For these reasons, the Stop-signal task has broad external and translational validity (Verbruggen and Logan, 2008).

There is considerable evidence suggesting that the inhibition or suppression of a motor response relies upon a right-lateralized fronto-basal-ganglia circuit. Multiple neuroimaging studies of response inhibition using Go/No-Go and Stop-signal tasks have implicated a set of regions, including the right inferior frontal cortex (IFC), pre-supplementary association area (pre-SMA) and superior frontal gyrus, and structures of the basal ganglia, including the subthalamic nucleus (STN)(Aron and Poldrack, 2006; Aron et al., 2007; Chamberlain et al., 2009; Garavan et al., 1999; Rubia et al., 2001), and these results are supported by lesion (Floden and Stuss, 2006; Aron et al., 2003), TMS (Chambers et al., 2006; Chen et al., 2009; van den Wildenberg et al., 2009), and DBS studies (Ray et al., 2009). Beyond stopping, there is evidence supporting the role that these regions play in regulating inhibitory control, such that the same regions responsible for stopping a response also modulate the speed-accuracy tradeoff in decision making. For example, activity in the right IFC, pre-SMA, and STN is correlated with conflict-related slowing in a selective Stop-signal task (Aron et al., 2007) and activity in STN neurons has been shown to control the switch from automatic to volitional saccades in macaque monkeys (Isoda and Hikosaka, 2008). In addition, in Parkinson's patients, STN disruption leads to impaired decision-making in high conflict conditions, suggesting that the STN acts to raise the response threshold in the face of conflict (Frank et al., 2007).

Some previous studies have reported relationships between individual differences in stopping ability and fMRI signals. Negative correlations between activation during inhibition and SSRT (reflecting a positive relation between activation and stopping ability) have been observed in a number of regions including the right IFC and right STN (Aron and Poldrack, 2006), the left superior frontal gyrus (SFG) and left precentral gyrus (Li et al., 2006), as well as the pre-SMA and caudate (Li et al., 2008). However, other studies have reported greater activation in the bilateral STN, right globus pallidus, and bilateral putamen in individuals with longer SSRT during successful stopping (Li et al., 2008). Although there is some support for a relationship between neural activation and individual differences in go trial performance (Garavan et al., 2006), the relationship between activation and individual differences in response execution has received less attention.

As previously stated, one potential problem with previous studies is that they have used mass univariate (voxelwise) analyses (which require correction for multiple comparisons) along with relatively small sample sizes, which together result in very low power to detect correlations (Yarkoni, 2009). An alternative to this approach, which we utilize here, is to reduce the dimensionality of the dataset and then perform correlational analyses on the reduced data. A common method for dimensionality reduction with fMRI data is ICA (Calhoun et al., 2009; McKeown and Sejnowski, 1998; Beckmann and Smith, 2004). This method decomposes an fMRI dataset into a set of (temporally or spatially) independent components that are combined to produce an approximation to the observed data.

In the present study, we used the probabilistic ICA approach (Beckmann and Smith, 2004) as implemented in the MELODIC toolbox within the FSL software suite (Smith et al., 2004). Although ICA is usually applied to fMRI timeseries, here we apply it to a set of individual activation maps; thus, it identifies spatially independent components along with the loading on each of those components for each individual (see Smith et al. (2009) for a similar approach) while also allowing for condition-specific analyses. These loading coefficients, rather than raw voxel values, thus serve as the data to be related to behavior. In particular, rather than correlating behavior and raw voxel values for each person, repeated across all voxels in the brain, we correlated behavior with the loading coefficient for each subject (the subset of voxels that make up a given component). By greatly reducing the number of comparisons to be performed, this approach reduces multiple comparison issues and allows more powerful detection of brain/behavior correlations.

Methods

Samples

Raw data were included from five separate fMRI studies conducted on two scanners at the University of California, Los Angeles, each of which included two Stop-signal scan sessions administered in rapid event-related designs. While each study had its own additional inclusion and exclusion criteria (see below), all samples included right-handed healthy English-speaking subjects, free of neurological or psychiatric history, not currently taking psychoactive medication, with normal or corrected-to-normal vision and with no counter-indications for MRI (i.e., not claustrophobic, not pregnant, no metal in their bodies). Exclusion criteria for the current analysis included excessive motion during scanning, being under the age of 18, incomplete scan data, and poor task performance on all possible sessions (defined a priori as a response rate on Go trials of less than 75%, more than 10% incorrect Go trials, percent inhibition on Stop trials of less than 25% or greater than 75%, or a SSRT of less than 50 ms). Of the data acquired, 13 participants were excluded from our analyses due to technical issues (2; no or poor high-resolution anatomical image collected), excessive motion (7; more than one translational displacement of 3mm or greater), or poor performance (4). The final sample included a total of 126 participants. All participants gave written informed consent according to the procedures approved by the University of California Los Angeles Institutional Review Board.

All participants in each of the five studies performed a Stop-signal task (Logan, 1994). In this task, participants viewed a series of go stimuli (left- or rightwards-pointing arrows in the center of the screen) and were told to press a left or right button, respectively, in response to the stimulus. On a subset of trials (25% of all trials, fixed at one in every four trials), a stop signal was presented at a short delay after the go stimulus had appeared (an auditory signal for all included studies), in which case they were instructed to withhold their response. The delay of the onset of the stop signal, or stop signal delay (SSD), was varied, such that it was increased after the participant successfully inhibited in response to a stop-signal (making the next stop trial more difficult), and decreased after the participant failed to inhibit in response to a stop-signal (making the next stop trial less difficult). This one-up/one-down tracking procedure ensured that subjects successfully inhibited on approximately 50% of inhibition trials. As a result, difficulty level is individualized across subjects and both behavioral performance and numbers of successful stop trials are equated across subjects.

All studies included in the present analysis used a tracking Stop-signal task or a modification of the task (see Study 5 below). For all studies, the SSD for each stop trial was selected from one of two or four interleaved staircases (see below), with each SSD increasing or decreasing by 50 ms according to whether or not the participant successfully inhibited on the previous

stop trial, for that respective ladder. For subsequent runs, the last SSD of each staircase on the previous run was used as each staircase's starting value.

In all studies included in the present analysis, trials began with a white circular fixation ring in the center of the screen for 500 ms. Jittered null events were imposed between every trial, with the duration of the null event sampled from an exponential distribution (null events ranged from 0.5 to 4 s, with a mean of 1 s). Go trials began with the appearance of a white left-or rightwards pointing arrow within the fixation circle and ended after 1 s or until the participant responded, followed by the null period. Stop trials were identical to Go trials, except for the onset of the stop-signal after a variable SSD, which was a tone (900 Hz). If the participant inhibited their response, the stimuli remained on the screen for 1 s; if the participant responded, the arrow and fixation circle disappeared for the remaining time, followed by the jittered null period.

All participants received brief training on the Stop-signal task directly before scanning, and were instructed to inhibit responses on trials in which the stop-signal appears. Subjects were told that correctly responding and inhibiting were equally important. All participants responded with their right hands on a MR-compatible button box in the scanner, and stop tones were played through headphones. All participants performed two sessions of the task in the scanner (96 Go trials and 32 Stop trials per session).

Participants and tasks

Study 1—Sample one includes data from 55 healthy young adult participants (29 males; mean age, 19.35 (1.06 SD) years). In addition to the exclusion criteria listed above, exclusion criteria for study participation included an age of less than 14 or greater than 21, history of seizure disorder, and treatment with prescription drugs. Only those individuals aged 18 or over were included in the present analysis. For this version of the task, the SSD for each stop trial was selected from one of two interleaved staircases, each starting with SSD values of 200 and 320 ms.

Study 2—Sample two includes data from 28 healthy participants (18 males; mean age, 20.89 (3.19 SD) years). In addition to the exclusion criteria listed above, exclusion criteria for study participation included an age of less than 18 or greater than 40, current use of an illegal substance, and not having a social security number (for payment). For this version of the task, participants first performed a first run of the task outside of the scanner, and the SSD for each stop trial was selected from one of two interleaved staircases, each starting with SSD values of 250 and 350 ms.

Study 3—Sample three includes data from 15 healthy participants (9 males; mean age, 25.60 (5.46 SD) years). Exclusion criteria for study participation were as listed above. For this version of the task, the SSD for each stop trial was selected from one of four interleaved staircases, each starting with SSD values of 100, 150, 200, and 250 ms. For additional details on this study, see Aron and Poldrack (2006).

Study 4—Sample four includes data from 14 healthy participants (7 males; mean age, 24.14 (4.13 SD) years). Participants from study 4 were recruited as part of a larger study examining cortico-striatal functioning in typically developing children and siblings of probands with childhood onset schizophrenia. Participants included in the present analysis only included typically developing adults. In addition to the exclusion criteria listed above, exclusion criteria for study participation included a history of CNS disease and presence of a learning disability. For this version of the task, participants first performed a first run of the task outside of the

scanner, and the SSD for each stop trial was selected from one of two interleaved staircases, each starting with SSD values of 200 and 320 ms.

Study 5—Sample five includes data from 14 healthy participants (6 males; mean age, 23.21 (6.15 SD) years). Exclusion criteria for study participation were as listed above. Stimuli and timing of the Stop-signal task followed the above description, except for two differences. First, the stimuli remained on the screen for 1 s whether or not the participant responded. Second, the SSD values were generated according to SSD estimated in behavioral testing beforehand, where participants completed 320 trials (240 Go and 80 Stop trials) of a tracking Stop-signal task. From behavioral testing, a central SSD (SSDc) was computed by averaging values from the last 10 moves of 4 interleaved staircases. For scanning, 8 SSD values for each session were taken from the following: SSDc − 60 ms, SSDc − 20, SSDc + 20, and SSDc + 60, and 50 ms increases/decreases. For additional details on this study, see Xue et al. (2008).

Imaging Parameters

Data from Studies 1-2 were collected using a 3T Siemens Trio MRI scanner; data from studies 3-5 were collected using a 3T Siemens AG Allegra MRI scanner. For each run, 182 functional T2*-weighted echoplanar images (EPIs) were collected with the following parameters: slice thickness = 4 mm, 34 slices, time repetition (TR) = 2 s, time echo (TE) = 30 ms, flip angle = 90°, matrix 64 × 64, field of view (FOV) = 192 mm (33 slices and field of view (FOV) = 200 mm for Studies 3-5). Additionally, a T2-weighted matched-bandwidth high-resolution anatomical scan (same slice prescription as EPI) and MPRAGE were acquired. For studies 1-2, the parameters for MPRAGE were: TR = 1.9 s, TE = 2.26 ms, FOV = 250, matrix = 256 × 256, saggital plane, slice thickness = 1mm, 176 slices. For studies 3-5, the parameters for MPRAGE were: TR = 2.3 s, TE = 2.1 ms, FOV = 256, matrix = 192 × 192, saggital plane, slice thickness = 1mm, 160 slices. Stimulus presentation and timing of all stimuli and response events was achieved using Matlab (Mathworks) and the Psychtoolbox (www.psychtoolbox.org) on an Apple Powerbook running Mac OS 9 (Apple Computers, Cupertino, CA) for Studies 1-4, and on an IBM laptop for Study 5.

Data Analysis

Behavioral Data Analysis—Data were analyzed similarly across all studies despite slight differences in study design and imaging parameters. The mean, median and standard deviation of reaction time on Go trials were calculated only for Go trials in which participants correctly responded. Stop successful trials included only Stop trials on which participants successfully inhibited a response, and Stop unsuccessful trials included only Stop trials on which participants responded. Average SSD was calculated from SSD values across staircases. SSRT was estimated using the quantile method, which does not require an assumption of 50% inhibition (Band et al., 2003). In order to calculate SSRT according to the quantile method, all RTs on Go trials were arranged in ascending order, and the RT corresponding to the proportion of failed inhibition was selected. The average SSD was then subtracted from this quantile RT, providing an estimate of SSRT. One-way analyses of variance were conducted in order to examine differences in task performance between the five samples.

fMRI Data Analysis—Analyses were performed using tools from the FMRIB software library (www.fmrib.ox.ac.uk/fsl), version 4.1. The first two volumes from each scan were discarded to allow for T1 equilibrium effects. For each scan, images for each participant were realigned to compensate for small head movements (Jenkinson and Smith, 2001). Data were spatially smoothed using a 5 mm full-width-half-maximum Gaussian kernel. The data were filtered in the temporal domain using a nonlinear high-pass filter with a 66 s cutoff. A three-step registration process was used in which EPI images were first registered to the matched-bandwidth high-resolution scan, then to the MPRAGE structural image, and finally into

standard (Montreal Neurological Institute (MNI)) space, using affine transformations (Jenkinson and Smith, 2001).

Standard model fitting was conducted for all studies. The following events were modeled after convolution with a canonical double gamma hemody-namic response function: Go, StopInhibit, StopRespond, and nuisance events consisting of incorrect Go trials. Null events were not modeled and therefore constitute an implicit baseline. Events were modeled at the time of stimulus (arrow) onset with a duration of 1.5 s. Temporal derivatives and the six motion parameters were included as covariates of no interest to improve statistical sensitivity. For each subject, for each scan, StopInhibit-Go, StopInhibit-StopRespond, Go-Null, and Go-StopRespond contrasts were computed.

A second-level fixed-effects analysis was performed to average across scan sessions for each subject. The output from the fixed-effects analysis were then analyzed using a mixed-effects model with FLAME. For all higher-level analyses, study membership was modeled in order to control for potential differences across the five studies. Higher-level analyses included group-level StopInhibit-Go, StopInhibit-StopRespond, Go-Null, and Go-StopRespond contrasts. The following whole-brain regression analyses were conducted: SSRT on StopInhibit-Go, SSRT on StopInhibit-StopRespond, median Go RT on Go-Null, and SD Go RT on Go-Null. Group level statistics images were thresholded with a cluster-forming threshold of $z > 2.0$ and a cluster probability of $p < 0.05$, corrected for whole-brain multiple comparisons using Gaussian random field theory. The search region included 213,957 voxels. Brain regions were identified using the Harvard-Oxford cortical and subcortical probabilistic atlases, and all activations are reported in MNI coordinates.

ICA was carried out using Probabilistic Independent Component Analysis (Beckmann and Smith, 2004) as implemented in MELODIC Version 3.09, part of FSL (FMRIB's Software Library, www.fmrib.ox.ac.uk/fsl). Group ICA was applied to the contrast images obtained from StopInhibit-Go, StopInhibit-StopRespond, and Go-Null contrasts, after adding 1000 to all in-mask voxels to ensure positive values for subsequent analyses. The number of components specified in ICA determines the level of homogeneity within, and heterogeneity between, networks and it has been demonstrated that a network dimensionality threshold of 20 matches many previous analyses of resting state data; in particular, 10 of these 20 components have been shown to be unambiguously paired between brain activation and resting scan data sets (Smith et al., 2009). A higher threshold results in more components that represent sub-networks (Smith et al., 2009), while a lower threshold potentially results in less homogenous networks. We therefore chose an ICA threshold of 20 (following Smith et al. (2009)) in order to isolate relatively homogeneous networks. We also ran Group ICA with a threshold of 10 and 30 components, and were able to identify similar components as those identified with a threshold of 20.

Group ICA resulted in 20 components, for each of the three contrasts examined, with a loading coefficient in each of the 20 components for each subject. This value reflects a subject's loading on that component, which indicates for that contrast the relative activity across the subset of voxels comprising that component. The relationship between performance measures (SSRT, Median Go RT, SD of Go RT) and the loading for each subject on each of the 20 independent components was modeled using linear regression, with a separate mean modeled for each study (see Figure 1). Regressions were conducted for independent components from StopInhibit-Go and StopInhibit-StopRespond against SSRT, and for components from Go-Null against Median Go RT and SD of Go RT. Because the component scores were correlated across different components, P-values corrected for multiple comparisons (for the 20 components) were obtained using permutation testing by computing the maximum t-statistic under the null. 10,000 permutations were used, and the five studies were treated as exchangeability blocks, such that

samples were only permuted within each study. Finally, in order to assess the amount of variance in SSRT that these components account for, we conducted a multiple linear regression.

For visualization of results, statistical maps were projected onto an average cortical surface with the use of multifiducial mapping using CARET software (Van Essen, 2005). For reporting of clusters within components of interest, we thresholded individual components at increased thresholds (2.58) to produce separate clusters using the cluster command in FSL. Anatomical localization within each cluster was obtained by searching within maximum likelihood regions from the FSL Harvard-Oxford probablistic atlas to obtain the maximum Z statistic and MNI coordinates within each anatomical region contained within a cluster.

Results

Behavioral Results

Behavioral data from all participants included in the present analysis (N = 126) are presented in Table 1. The tracking procedure of the Stop-signal task worked similarly across all studies using the tracking procedure (studies 1-4). As demonstrated in the behavioral performance reported in Table 1, correct responding on Go trials was close to 100% in all studies, and the inhibition rate was close to 50% in all studies, reflecting successful employment of the tracking procedure. Neither median RT nor the standard deviation (SD) of RT on Go trials was correlated with SSRT. One-way analyses of variance to test for differences in task performance between the five samples (data not shown) revealed no difference in SSRT or Median Go RT between the five samples, although there was a significant difference in the SD of Go RT between the five samples ($F(1, 124) = 15.84$, $p < 0.001$).

fMRI Results: Whole-brain activation

Inspection of activation from the StopInhibit-Go contrast revealed activation commonly seen during response inhibition, including activation in the right inferior frontal/frontal opercular/insular cortices that extended to the frontal pole, right middle frontal and precentral gyri, and medial preSMA through the SFG (see Supplementary Figure 1). In particular, there was bilateral activation in the anterior insula and frontal operculum, but this activation extended through the IFC in the right hemisphere. Activation was also seen in the posterior cingulate, basal ganglia (particularly the bilateral caudate), right thalamus, bilateral posterior clusters (supramarginal and angular gyri) through the temporal cortex, and visual cortex. This pattern of activation replicates that previously seen in studies using auditory Stop-signal tasks.

Inspection of activation from the Go-Null contrast when combining data across five studies, while controlling for group membership, revealed significant activation in a motor pathway (see Supplementary Figure 1). In addition to activation throughout posterior regions, including the occipital cortex and cerebellum, activation during successful Go trials was seen in the thalamus and basal ganglia, the SMA through the pre-SMA and cingulate, and the motor cortex. This pattern of activation is expected for a task with a visual stimulus and hand motor response. This pattern was also largely contralateral, which is to be expected as every participant produced a right-handed response.

Inspection of activation from the StopInhibit-StopRespond contrast also revealed activation seen during stopping, including activation in the right precentral gryus/SFG/MFG extending into the postcentral gyrus/superior parietal lobule/supramarginal and angular gyri and bilateral lateral occipital cortex/occipital pole (see Supplementary Figure 2). Activation was also seen throughout the bilateral striatum, as well as the bilateral amygdala and hippocampus. In contrast, inspection of activation from the StopRespond-StopInhibit contrast revealed localized

activation in the left postcentral gyrus extending into the parietal and central opercular cortices, presumably reflecting motor execution processes (see Supplementary Figure 2).

Although both Go and StopRespond trials include a motor response, inspection of activation from the Go-StopRespond contrast continued to reveal activation in a motor regions, including bilateral pre- and postcentral gyri, while there was no activation in the motor cortex in the StopRespond-Go contrast at corrected levels (see Supplementary Figure 3). Additional activation in the Go-StopRespond contrast was seen in the left middle and superior frontal gyrus, bilateral supramarginal gyrus, bilateral superior parietal lobule and lateral occipital cortex into frontal orbital cortex and occipital pole, and bilateral putamen. Activation was also seen in the frontal medial cortex and paracingulate into the frontal pole, the precuneus and posterior cingulate, as well as the bilateral hippocampus and amygdala, parahippocampal gyrus and temporal fusiform cortex.

Inspection of activation in the StopRespond-Go contrast revealed significant activation in the posterior through the anterior cingulate and paracingulate, pre-SMA, and bilateral superior frontal gyrus, extensive bilateral parietal and temporal activation, including activation in the auditory cortex, posterior activation limited to the intracalcarine cortex, and activation in the bilateral caudate and thalamus. Activation was also seen in the bilateral IFC/operculum/insula and precentral gyrus, extending into the frontal ortbital cortex and, in the right hemisphere, this activation extended through the precentral gyrus, middle frontal gyrus and frontal pole.

fMRI Results: Whole-brain behavioral correlations

StopInhibit-Go and SSRT—At whole-brain corrected levels, there were no regions of activation that negatively correlated with SSRT. Lowering the threshold to $p < 0.005$ (uncorrected) revealed clusters in the pre-SMA/SFG/paracingulate, the right IFC and frontal operculum, and bilateral frontal orbital/insular cortices that negatively correlated with SSRT (see A in Figure 2). At whole-brain corrected levels, SSRT positively correlated with activation in the precuneus cortex/posterior cingulate gyrus and the frontal medial cortex/paracingulate/anterior cingulate gyrus, as well as bilateral precentral/postcentral gyri/SMA and bilateral putamen (see B in Figure 2).

StopInhibit-StopRespond and SSRT—At whole-brain corrected levels, there were no regions of activation that negatively correlated with SSRT. Lowering the threshold to $p < 0.005$ (uncorrected) revealed small clusters in the right pre-SMA, right frontal pole, right IFC/insular cortex, left frontal orbital cortex, and anterior cingulate cortex that negatively correlated with SSRT (see C in Figure 2). At whole-brain corrected levels, SSRT positively correlated with activation in the right postcentral gyrus, parietal and central opercular cortices, and planum temporale (see D in Figure 2).

Go-Null and RT on Go trials—At whole-brain corrected levels, there were no regions of activation that correlated with median or SD of Go RT. Lowering the threshold to $p < 0.005$ (uncorrected) revealed regions in the left precentral gyrus, bilateral lateral occipital cortex, and bilateral caudate that negatively correlated with median Go RT (see E in Figure 2). For Go RT SD at the lower threshold, there was a significant negative correlation in the left postcentral gyrus, left superior parietal lobule, left supramarginal gyrus, bilateral lateral occipital cortex, left posterior cingulate, right lingual gyrus, right caudate and left amygdala (see F in Figure 2). There were no regions of activation that positively correlated with median or SD of Go RT at uncorrected levels.

fMRI Results: Group ICA

For StopInhibit-Go, StopInhibit-StopRespond, and Go-Null contrasts, 20 independent components were specified using MELODIC. These components represent spatially independent patterns of activation present in each contrast. The ICs revealed by MELODIC were consistent with the whole-brain analyses, but they separate the overall activation map into a number of different components, and also identify some networks that were not activated by the task. The components that were significantly related to behavioral performance after correction for multiple testing are reported here and presented in Tables 2-3 and Figures 3-4. These maps reflect the loading of each voxel on each independent component, which are estimated across all subjects.

StopInhibit Components and SSRT—In the complete sample of healthy adults, four components of activation significantly correlated with SSRT. SSRT negatively correlated with two components, each of which included widespread activation in regions generally associated with stopping. Component 14 ($t = -3.35$, $p < 0.005$) survived correction for multiple comparisons ($p_{corr} < 0.05$) (see Table 2 and Figure 3), and was associated with greater activity in the pre-SMA/SFG/paracingulate cortex through the ACC, bilateral IFC/frontal opercular/insular cortices, and the bilateral striatum, pallidum, and thalamus.

Component 2 ($t = -2.95$, $p < 0.01$), did not survive correction for multiple comparisons ($p_{corr} = 0.09$) (see Table 2 and Figure 3). It was associated with activation in the right IFC/frontal opercular/insular/frontal orbital cortices that extended into the MFG/frontal pole, the pre-SMA/SFG/paracingulate cortex, left MFG, posterior cingulate, right angular gyrus/supramarginal/lateral occpital cortices, and the right thalamus.

SSRT positively correlated with component 1 ($t = 3.29$, $p < 0.005$), which survived correction for multiple comparisons ($p_{corr} < 0.05$) and represented activation in what has been labeled the “default mode” network, including the anterior paracingulate gyrus/subcallosal cortex/frontal pole/frontal medial cortex, the precuneus/posterior cingulate, bilateral hippocampus/parahippocampal gyrus/temporal occipital fusiform cortex and bilateral lateral occipital cortex (see Table 3 and Figure 4).

SSRT also positively correlated with component 9 ($t = 2.79$, $p < 0.01$), which did not survive correction for multiple comparisons ($p_{corr} = 0.14$) and was associated with activation in regions involved in motor planning and execution (see Table 3 and Figure 4). In particular, this component consisted of activation in the SMA/bilateral precentral and postcentral gyri, posterior cingulate gyurs, and the left putamen.

We conducted a multiple linear regression, with these four components predicting SSRT in our sample of 126 adults. Together, the four components accounted for 7% of the variance in SSRT scores. When controlling for the influence of other independently significant components, only Component 14 showed a significant partial correlation with SSRT ($p < 0.05$).

Only components from the StopInhibit-Go contrast were significantly correlated with SSRT. Although we also examined the relationship between SSRT and activation during StopInhibit trials, as compared to StopRespond trials, none of the components were significantly related to SSRT after correction for multiple comparisons (corrected p values > 0.08).

Go Components and Go RT—We also examined the relationship between activation during Go trials and both median and SD of Go RT. Although the independent components identified by Group ICA were consistent with the results from the whole-brain contrasts, none of the components were significantly related to either median or SD of Go RT after correction for multiple comparisons (corrected p values > 0.3).

Discussion

The present results clearly demonstrate that brain/behavior correlation analyses benefit from the use of dimensionality reduction in comparison to voxelwise analyses. In particular, we found that whereas voxelwise analyses with appropriate statistical corrections did not detect robust correlations between behavior and activation, even in a well-powered sample, significant correlations were detected between behavior and activation in a set of distributed networks identified using independent components analysis. When ICA was applied to statistical maps (rather than timeseries), it provided a set of components that were strongly concordant with results from previous voxelwise analyses, including components that reflect networks commonly associated with motor response execution and also regions known to be critical for response inhibition. It also identified regions that are commonly deactivated during task performance, including the midline regions commonly known as the “default mode” network (Raichle et al., 2001).

Analyses of the correlation between engagement of these components and behavioral measures of response inhibition provide a resolution to inconsistencies in previous studies of the relation between inhibitory control behavior and fMRI signals. First, our results demonstrate that response inhibition ability is positively related to engagement of networks that include regions that have been consistently shown to be active in the Stop-signal paradigm, including right IFG/anterior insula, pre-SMA, and basal ganglia structures. These findings are highly consistent with previous reports not only of activation seen during successful inhibition during performance of the Stop-signal task, but also with previous reports of the relationship between activation in these regions and individual differences in performance across stopping tasks (Forstmann et al., 2008; Goghari and MacDonald, 2009; Li et al., 2006, 2008). Second, our results demonstrate that response inhibition ability is negatively related to the engagement of the default mode network across individuals.

A novel aspect of the present results is the significant association between response inhibition ability and components derived from ICA applied to statistical maps, although the activation in stopping-related components is in line with previous reports. Component 14 included key regions associated with response inhibition, including the pre-SMA/SFG/paracingulate, the right IFC/opercular/insular cortices, and bilateral basal ganglia and thalamus. Component 2 included these same regions, but also included the right frontal orbital cortex/MFG/frontal pole, left MFG, posterior cingulate, and right posterior parietal through occipital cortex. The correlation between SSRT and activation in component 14 was significant, even after correction for multiple comparisons, further demonstrating that the regions included in component 14 represent critical regions underlying response inhibition. Results of our voxel-wise regression analyses revealed activation in many of these same regions, although at an uncorrected threshold, providing tentative evidence of whole-brain correlations. These findings are consistent with previous imaging studies that have taken both whole-brain and region of interest approaches, as well as results from DTI analyses (Aron et al., 2007; Li et al., 2006, 2008) and loss-of-function studies (Aron et al., 2003; Chambers et al., 2006; Chen et al., 2009; Floden and Stuss, 2006).

The use of component-based analysis also allowed us to find interesting negative relationships between brain activity and inhibitory performance. First, SSRT positively correlated with activation in the default mode network, which was identified from task activation maps through the use of ICA. The default-mode network comprised a network of brain regions, including the medial prefrontal cortex, the medial, lateral, and inferior parietal cortex, and the precuneus/posterior cingulate cortex, which are consistently deactivated during performance of cognitive tasks and activated during rest (Biswal et al., 2010; Raichle et al., 2001).

Our ICA analysis of Stop-signal data revealed distinct components of activation throughout the default-mode network for both StopInhibit-Go and Go-Null contrasts. However, only default-mode network activation during successful Stop trials positively correlated with SSRT. This is an intriguing finding and is in line with suggestions that increased default-mode network activity during task performance may underlie impaired attentional control (Mason et al., 2007; Sonuga-Barke and Castellanos, 2007). As an increase of activation, or an attenuation of deactivation, in this network is suggested to interfere with task-specific attention and goal-directed action, our finding of a positive correlation between default-mode network activation and SSRT suggests that default-mode network activation in individuals with poorer response inhibition may reflect another mechanism of impaired response inhibition. Alternatively, the relative engagement of default mode versus task-related components may reflect the degree to which each subject is cognitively engaged in the task.

Second, SSRT positively correlated with activation in a motor pathway, including the SMA through bilateral pre- and postcentral gyri, the posterior cingulate, and the left putamen. Although this correlation did not survive correction, it is suggestive that individuals with poorer response inhibition (longer SSRT) had increased activation in regions responsible for the execution of a motor response in comparison to individuals with better response inhibition. It has been reported in a TMS study that successful Stop trials are associated with suppression of cortico-motoneuronal excitability as compared to baseline (Badry et al., 2009). An incomplete motor suppression response may therefore represent another potential mechanism influencing poor response inhibition.

It is interesting that only the correlations between components from the StopInhibit-Go contrast and SSRT survived correction. Although there were significant correlations between go-task performance and components of go-task activation, these did not survive correction. There is a considerable body of evidence supporting the relationship between individual differences in stopping activation and performance, specifically in the right IFC, preSMA, and right STN, and much less supporting a relationship between individual differences in going activation and performance. However, there is reason to expect to see a relationship between performance on Go trials and neural activation. For example, a negative correlation between Go RT and bilateral insula activation during successful Stop trials has been reported (Garavan et al., 2006). The reason for specificity of correlations between stopping activation and performance may be that there is greater variability associated with the neural mechanisms underlying the response inhibition as opposed to execution.

The components extracted from the StopInhibit-StopRespond contrast also did not correlate with performance after correction. This reflects the substantial overlap in the engagement of the right-lateralized fronto-basal ganglia network between StopInhibit and StopRespond trials. We have focused on the StopInhibit-Go contrast because this is the contrast that should most directly index inhibitory function according to the race model of stop-signal inhibition. Although it is not immediately intuitive, the difference between StopRespond and StopInhibit trials in the stop signal task is not actually thought to reflect differences in inhibition according to this model. Rather, it should instead reflect differences in the speed of the Go process that is racing against the Stop process.

Consistent with our analyses of ICA components, activation during StopInhibit-StopRespond that negatively correlated with SSRT did not survive correction in our voxel-wide analyses. In contrast, the activation during StopInhibit-StopRespond that positively correlated with SSRT did survive correction. Although one might interpret this difference in findings from ICA vs. voxel-wise analyses as reflecting the sensitivity of ICA to broad vs. specific constructs, respectively, we believe that the lack of significant correlations between StopInhibit-StopRespond components and SSRT instead reflects the limited set of regions for the

StopInhibit-StopRespond (or StopRespond-StopInhibit) comparison, combined with the use of a relatively small number of independent components, which biases the analysis towards finding broader components.

A strength of the present study is that we used Group ICA to analyze functional imaging data acquired during the performance of a Stop-signal task in a large sample of healthy adults. An advantage of using Group ICA to isolate components, which we can then correlate with task performance, is that we are able to tease apart patterns of activation in regions that would otherwise not be distinct in group-level activation maps. A common approach is to compare successful Stop trials to successful Go or unsuccessful Stop trials in an attempt to isolate activation specific to the stopping process. Both of these contrasts, however, involve more than just response inhibition. For example, for successful Stop as compared to Go trials, there is the additional perceptual processing associated with the stop-signal. Furthermore, this contrast still captures aspects of motor planning and processing. This is apparent in the results of our ICA analyses as component 9, which positively correlated with SSRT, included widespread activation in a motor planning and execution network. It is also noteworthy that we were able to identify activation in the "default-mode" network (component 1) even though we analyzed statistical maps, as opposted to timeseries data.

An additional strength of this analysis is that we were able to take advantage of data collected across five separate studies and combine them into one mega-analysis (Costafreda, 2009). Rather than combining results from separate studies, we were able to combine the data and perform a new series of analyses. Furthermore, even though different scanners were used, we were able to control for group membership in our group-level analyses, as well as in our correlations, in order to control for scanning- and study-related differences.

Indeed, we believe that a particular strength of our study is the sufficiently large sample size needed in order to compare this data dimensionality reduction approach to mass univariate analyses for the purposes of individual differences research. One of the main reasons for the inconsistency in results regarding the relationship between inhibitory control (or better yet, any measure of individual differences) and fMRI signals has been the use of small samples with low power to detect correlations of reasonable size. It has become increasingly clear that sample sizes on the order of 100 subjects are necessary in order to obtain sufficient power to find correlations of reasonable size (e.g., Yarkoni (2009)). As such, our sample is novel in demonstrating the nature of SSRT-activation correlations in a well powered sample and likely more accurately reflects the relationship between individual differences in performance and activation than previously reported.

We did limit our sample to only include individuals over the age of 18. Age has been shown to have a significant influence not only on Stop-signal performance, but also on neural activation during response inhibition (Bunge et al., 2002; Rubia et al., 2006). Indeed, there is reason to believe that the brain regions underlying successful response inhibition are not yet fully matured and are still undergoing cortical differentiation before the age of 18 and therefore drastically alter patterns of activation as compared to adults. Furthermore, SSRT has been reported to decrease with age (Williams et al., 1999; Ridderinkhof et al., 1999). Our results are therefore specific to adults and the relationship between components from Group ICA and performance may differ considerably in children and adolescents.

These results do not directly speak to the debate over whether the right IFC is directly involved in the suppression of a motor response as part of a hyperdirect pathway (Aron, 2007; Swann et al., 2009), or whether the right IFC plays a signal monitoring role (Chao et al., 2009). These results do however highlight the extent of activation seen throughout a right frontal cluster which includes activation in the IFC, frontal operculum, insula, frontal orbital cortex, and

frontal pole. In line with this, it has been reported that right inferior frontal activation during complete response inhibition did not overlap with inferior frontal activation while preparing to inhibit an upcoming automatic response (Goghari and MacDonald, 2009). In the present study, we found that activation in one component from the StopInhibit-Go contrast was significantly correlated with SSRT after correction, while another was not, even though both included overlapping activation in right frontal, as well as superior frontal and paracingulate, regions. The amount and degree of activation seen in these regions is large, and further work will be needed to attempt to identify the roles within each of these regions during response inhibition.

Conclusion

The present study was designed to examine components of activation using Group ICA in a large sample of healthy adults performing a Stop-signal task and to examine the relationship between components of activation and performance. Although there have been previous attempts to elucidate the relationship between inhibitory ability and brain activation, the results of these analyses were not conclusive. An advantage, and novel aspect, of our study is that we analyzed a sufficiently large data set in order to better elucidate the relationship between individual differences in performance and neural activation. By conducting our analyses in a large sample, our results potentially reveal a more accurate and complete picture of this relationship than has previously been reported. In doing so we were also able to contrast the use of mass univariate analyses with the powerful approach of correlating behavior with components extracted from Group ICA. Although we found activation throughout a right-lateralized stopping network during successful Stop trials and throughout a motor pathway during successful Go trials (consistent with previous reports), our use of Group ICA allowed us to identify multiple neural mechanisms underlying individual differences in inhibitory ability. In contrast, our whole-brain correlation analyses did not survive correction, even in a sample of 126 adults, illustrating the limitation of this mass univariate approach. In particular, we identified a component of activation, including a large right inferior frontal cluster, a pre-SMA/SFG/paracingulate cluster, the basal ganglia and thalamus, which negatively correlated with SSRT. We also identified a component of activation representing the default-mode network which positively correlated with SSRT.

The different relationships between brain activation and performance suggest multiple possible mechanisms which may influence why individuals are less able to inhibit a motor response than others. These results clearly show a relationship between individual differences in stopping ability in specific activated networks, including regions known to be critical for the behavior, and highlight the usefulness of using independent components analysis of imaging maps to increase the power to detect brain/behavior correlations in individual differences research. Further work will be needed to examine these components and their relative relationships to individual differences in response inhibition, as well as the relationship between these components and performance in highly impulsive samples or other samples characterized by impaired inhibitory control. Understanding this relationship between individual differences in performance and neural activation has implications for a number of psychiatric populations characterized by deficits in inhibitory control, as it offers the possibility of identifying etiological mechanisms of impairment that are putatively closer to genetic and environmental influence.

Supplementary Material

Refer to Web version on PubMed Central for supplementary material.

Acknowledgments

This work was supported by an NIH/NINDS training grant (T32 NS048004; N. Freimer, PI), and research grants from the NIH (PL1MH083271; R. Bilder, PI), Office of Naval Research (R. Poldrack, PI), and James S. McDonnell Foundation (R. Poldrack, PI).

References

Aron AR. The neural basis of inhibition in cognitive control. Neuroscientist 2007;13(3):214–228. [PubMed: 17519365]

Aron AR, Behrens TE, Smith S, Frank MJ, Poldrack RA. Triangulating a cognitive control network using diffusion-weighted magnetic resonance imaging (MRI) and functional MRI. J Neurosci 2007;27(14): 3743–3752. [PubMed: 17409238]

Aron AR, Fletcher PC, Bullmore ET, Sahakian BJ, Robbins TW. Stop-signal inhibition disrupted by damage to right inferior frontal gyrus in humans. Nat Neurosci 2003;6(2):115–116. [PubMed: 12536210]

Aron AR, Poldrack RA. Cortical and subcortical contributions to stop signal response inhibition: Role of the subthalamic nucleus. J Neurosci 2006;26(9):2424–2433. [PubMed: 16510720]

Avila C, Parcet MA. Personality and inhibitory deficits in the stop-signal task: The mediating role of Gray's anxiety and impulsivity. Personality and Individual Differences 2001;31(6):975–986.

Badry R, Mima T, Aso T, Nakatsuka M, Abe M, Fathi D, Foly N, Nagiub H, Nagamine T, Fukuyama H. Suppression of human cortico-motoneuronal excitability during the stop-signal task. Clin Neurophysiol 2009;120(9):1717–23. [PubMed: 19683959]

Band GPH, van der Molen MW, Logan GD. Horse-race model simulations of the stop-signal procedure. Acta Psychol (Amst) 2003;112(2):105–142. [PubMed: 12521663]

Beckmann CF, Smith SM. Probabilistic independent component analysis for functional magnetic resonance imaging. IEEE Trans Med Imaging 2004;23(2):137–52. [PubMed: 14964560]

Biswal BB, Mennes M, Zuo X-N, Gohel S, Kelly C, Smith SM, Beckmann CF, Adelstein JS, Buckner RL, Colcombe S, Do-gonowski A-M, Ernst M, Fair D, Hampson M, Hoptman MJ, Hyde JS, Kiviniemi VJ, Kötter R, Li S-J, Lin C-P, Lowe MJ, Mackay C, Madden DJ, Madsen KH, Margulies DS, Mayberg HS, McMahon K, Monk CS, Mostofsky SH, Nagel BJ, Pekar JJ, Peltier SJ, Petersen SE, Riedl V, Rombouts SARB, Rypma B, Schlaggar BL, Schmidt S, Seidler RD, Siegle GJ, Sorg C, Teng G-J, Veijola J, Villringer A, Walter M, Wang L, Weng X-C, Whitfield-Gabrieli S, Williamson P, Windischberger C, Zang Y-F, Zhang H-Y, Castellanos FX, Milham MP. Toward discovery science of human brain function. Proc Natl Acad Sci U S A Mar;2010 107(10):4734–9. [PubMed: 20176931]

Boucher L, Palmeri TJ, Logan GD, S. JD. Inhibitory control in mind and brain: An interactive race model of countermanding saccades. Psychological Review 2007;114(2):376–97. [PubMed: 17500631]

Bunge SA, Dudukovic NM, Thomason ME, Vaidya CJ, Gabrieli JDE. Immature frontal lobe contributions to cognitive control in children: Evidence from fMRI. Neuron 2002;33(2):301–11. [PubMed: 11804576]

Calhoun VD, Liu J, Adali T. A review of group ICA for fMRI data and ICA for joint inference of imaging, genetic, and ERP data. Neuroimage 2009;45(1 Suppl):S163–72. [PubMed: 19059344]

Chamberlain SR, Hampshire A, Müller U, Rubia K, Del Campo N, Craig K, Regenthal R, Suckling J, Roiser JP, Grant JE, Bullmore ET, Robbins TW, Sahakian BJ. Atomoxetine modulates right inferior frontal activation during inhibitory control: A pharmacological functional magnetic resonance imaging study. Biol Psychiatry 2009;65(7):550–5. [PubMed: 19026407]

Chambers CD, Bellgrove MA, Stokes MG, Henderson TR, Garavan H, Robertson IH, Morris AP, Mattingley JB. Executive “brake failure” following deactivation of human frontal lobe. J Cogn Neurosci 2006;18(3):444–455. [PubMed: 16513008]

Chambers CD, Garavan H, Bellgrove MA. Insights into the neural basis of response inhibition from cognitive and clinical neuroscience. Neurosci Biobehav Rev 2009;33(5):631–46. [PubMed: 18835296]

Chao HHA, Luo X, Chang JLK, Li C-SR. Activation of the pre-supplementary motor area but not inferior prefrontal cortex in association with short stop signal reaction time–an intra-subject analysis. BMC Neurosci 2009;10:75. [PubMed: 19602259]

Chen C-Y, Muggleton NG, Tzeng OJL, Hung DL, Juan C-H. Control of prepotent responses by the superior medial frontal cortex. Neuroimage 2009;44(2):537–545. [PubMed: 18852054]

Cools R. Role of dopamine in the motivational and cognitive control of behavior. Neuroscientist 2008;14 (4):381–395. [PubMed: 18660464]

Costafreda SG. Pooling fMRI data: Meta-analysis, mega-analysis and multi-center studies. Frontiers in Neuroinformatics 2009;3(33) Epub 2009 Sep 30.

Enticott PG, Ogloff JRP, Bradshaw JL. Associations between laboratory measures of executive inhibitory control and self-reported impulsivity. Personality and Individual Differences 2006;41(2):285–294.

Ersche KD, Roiser JP, Robbins TW, Sahakian BJ. Chronic cocaine but not chronic amphetamine use is associated with perseverative responding in humans. Psychopharmacology (Berl) 2008;197(3):421–431. [PubMed: 18214445]

Fillmore MT, Rush CR. Impaired inhibitory control of behavior in chronic cocaine users. Drug Alcohol Depend 2002;66(3):265–273. [PubMed: 12062461]

Fillmore MT, Rush CR. Polydrug abusers display impaired discrimination-reversal learning in a model of behavioural control. J Psychopharmacol 2006;20(1):24–32. [PubMed: 16174667]

Floden D, Stuss DT. Inhibitory control is slowed in patients with right superior medial frontal damage. J Cogn Neurosci 2006;18(11):1843–1849. [PubMed: 17069475]

Forstmann BU, Jahfari S, Scholte HS, Wolfensteller U, van den Wildenberg WPM, Ridderinkhof KR. Function and structure of the right inferior frontal cortex predict individual differences in response inhibition: A model-based approach. J Neurosci 2008;28(39):9790–6. [PubMed: 18815263]

Frank MJ, Samanta J, Moustafa AA, Sherman SJ. Hold your horses: Impulsivity, deep brain stimulation, and medication in Parkinsonism. Science 2007;318(5854):1309–1312. [PubMed: 17962524]

Friedman NP, Miyake A. The relations among inhibition and interference control functions: A latent-variable analysis. J Exp Psychol Gen 2004;133(1):101–135. [PubMed: 14979754]

Garavan H, Hester R, Murphy K, Fassbender C, Kelly C. Individual differences in the functional neuroanatomy of inhibitory control. Brain Res 2006;1105(1):130–42. [PubMed: 16650836]

Garavan H, Ross TJ, Stein EA. Right hemispheric dominance of inhibitory control: An event-related functional MRI study. Proc Natl Acad Sci U S A 1999;96(14):8301–8306. [PubMed: 10393989]

Goghari VM, MacDonald AW 3rd. The neural basis of cognitive control: Response selection and inhibition. Brain Cogn 2009;71(2):72–83. [PubMed: 19427089]

Isoda M, Hikosaka O. Role for subthalamic nucleus neurons in switching from automatic to controlled eye movement. J Neurosci 2008;28(28):7209–18. [PubMed: 18614691]

Jenkinson M, Smith S. A global optimisation method for robust affine registration of brain images. Med Image Anal 2001;5(2):143–56. [PubMed: 11516708]

Jentsch JD, Taylor JR. Impulsivity resulting from frontostriatal dysfunction in drug abuse: Implications for the control of behavior by reward-related stimuli. Psychopharmacology (Berl) 1999;146(4):373–390. [PubMed: 10550488]

Li C-SR, Huang C, Constable RT, Sinha R. Imaging response inhibition in a stop-signal task: Neural correlates independent of signal monitoring and post-response processing. J Neurosci 2006;26(1): 186–192. [PubMed: 16399686]

Li C-SR, Yan P, Sinha R, Lee T-W. Subcortical processes of motor response inhibition during a stop signal task. Neuroimage 2008;41(4):1352–1363. [PubMed: 18485743]

Lijffijt M, Kenemans JL, Verbaten MN, van Engeland H. A meta-analytic review of stopping performance in Attention-Deficit/Hyperactivity Disorder: Deficient inhibitory motor control? J Abnormal Psychology 2005;114(2):216–222.

Logan, GD. On the abillity to inhibit thought and action: A users' guide to the stop signal paradigm. In: Dagenbach, D.; Carr, TH., editors. Inhibitory Processes in Attention, Memory and Language. Academic Press; San Diego: 1994. p. 189-239.

Logan GD, Cowan WB. On the ability to inhibit thought and action: A theory of an act of control. Psychological Review 1984;91:295–327.

Logan GD, Schachar RJ, Tannock R. Impulsivity and inhibitory control. Psychological Science 1997;8 (1):60–64.

Mason MF, Norton MI, Van Horn JD, Wegner DM, Grafton ST, Macrae CN. Wandering minds: The default network and stimulus-independent thought. Science 2007;315(5810):393–5. [PubMed: 17234951]

McKeown MJ, Sejnowski TJ. Independent component analysis of fMRI data: Examining the assumptions. Hum Brain Mapp 1998;6(5-6):368–72. [PubMed: 9788074]

Monterosso JR, Aron AR, Cordova X, Xu J, London ED. Deficits in response inhibition associated with chronic methamphetamine abuse. Drug Alcohol Depend 2005;79(2):273–277. [PubMed: 15967595]

Nigg JT, Silk KR, Stavro G, Miller T. Disinhibition and borderline personality disorder. Dev Psychopathol 2005;17(4):1129–49. [PubMed: 16613434]

Oosterlaan J, Logan GD, Sergeant JA. Response inhibition in AD/HD, CD, comorbid AD/HD + CD, anxious, and control children: A meta-analysis of studies with the stop task. J Child Psychol Psychiatry 1998;39(3):411–25. [PubMed: 9670096]

Raichle ME, MacLeod AM, Snyder AZ, Powers WJ, Gusnard DA, Shulman GL. A default mode of brain function. Proc Natl Acad Sci U S A 2001;98(2):676–82. [PubMed: 11209064]

Ray NJ, Jenkinson N, Brittain J, Holland P, Joint C, Nandi D, Bain PG, Yousif N, Green A, Stein JS, Aziz TZ. The role of the subthalamic nucleus in response inhibition: Evidence from deep brain stimulation for Parkinson's disease. Neuropsychologia 2009;47(13):2828–34. [PubMed: 19540864]

Ridderinkhof KR, Band GPH, Logan GD. A study of adaptive behavior: Effects of age and irrelevant information on the ability to inhibit one's actions. Acta Psychologica 1999;101(2-3):315–337.

Rubia K, Russell T, Overmeyer S, Brammer MJ, Bullmore ET, Sharma T, Simmons A, Williams SC, Giampietro V, Andrew CM, Taylor E. Mapping motor inhibition: Conjunctive brain activations across different versions of go/no-go and stop tasks. Neuroimage 2001;13(2):250–261. [PubMed: 11162266]

Rubia K, Smith AB, Woolley J, Nosarti C, Heyman I, Taylor E, Brammer M. Progressive increase of frontostriatal brain activation from childhood to adulthood during event-related tasks of cognitive control. Hum Brain Mapp 2006;27(12):973–93. [PubMed: 16683265]

Rucklidge JJ, Tannock R. Neuropsychological profiles of adolescents with ADHD: Effects of reading difficulties and gender. J Child Psychol Psychiatry 2002;43(8):988–1003. [PubMed: 12455921]

Schachar R, Logan G. Are hyperactive children deficient in attentional capacity? J Abnorm Child Psychol 1990;18(5):493–513. [PubMed: 2266222]

Schachar RJ, Crosbie J, Barr CL, Ornstein TJ, Kennedy J, Malone M, Roberts W, Ickowicz A, Tannock R, Chen S, Pathare T. Inhibition of motor responses in siblings concordant and discordant for Attention Deficit Hyperactivity Disorder. Am J Psychiatry 2005;162(6):1076–1082. [PubMed: 15930055]

Smith SM, Fox PT, Miller KL, Glahn DC, Fox PM, Mackay CE, Filippini N, Watkins KE, Toro R, Laird AR, Beckmann CF. Correspondence of the brain's functional architecture during activation and rest. Proc Natl Acad Sci U S A 2009;106(31):13040–5. [PubMed: 19620724]

Smith SM, Jenkinson M, Woolrich MW, Beckmann CF, Behrens TEJ, Johansen-Berg H, Bannister PR, De Luca M, Drobnjak I, Flitney DE, Niazy RK, Saunders J, Vickers J, Zhang Y, De Stefano N, Brady JM, Matthews PM. Advances in functional and structural MR image analysis and implementation as FSL. Neuroimage 2004;23(Suppl 1):S208–19. [PubMed: 15501092]

Sonuga-Barke EJS, Castellanos FX. Spontaneous attentional fluctuations in impaired states and pathological conditions: A neurobiological hypothesis. Neurosci Biobehav Rev 2007;31(7):977–86. [PubMed: 17445893]

Swann N, Tandon N, Canolty R, Ellmore TM, McEvoy LK, Dreyer S, DiSano M, Aron AR. Intracranial EEG reveals a time- and frequency-specific role for the right inferior frontal gyrus and primary motor cortex in stopping initiated responses. J Neurosci 2009;29(40):12675–85. [PubMed: 19812342]

van den Wildenberg WPM, Burle B, Vidal F, van der Molen MW, Ridderinkhof KR, Hasbroucq T. Mechanisms and dynamics of cortical motor inhibition in the stop-signal paradigm: A TMS study. J Cogn Neurosci. 2009 2009 Apr 28. [Epub ahead of print].

Van Essen DC. A population-average, landmark- and surface-based (PALS) atlas of human cerebral cortex. Neuroimage 2005;28(3):635–62. [PubMed: 16172003]

Verbruggen F, Logan G. Response inhibition in the stop-signal paradigm. Trends Cogn Sci 2008;12(11):418–24. [PubMed: 18799345]

Verbruggen F, Logan GD. Models of response inhibition in the stop-signal and stop-change paradigms. Neurosci Biobehav Rev 2009;33(5):647–61. [PubMed: 18822313]

Williams BR, Ponesse JS, Schachar RJ, Logan GD, Tannock R. Development of inhibitory control across the life span. Developmental Psychology 1999;35(1):205–213. [PubMed: 9923475]

Xue G, Aron AR, Poldrack RA. Common neural substrates for inhibition of spoken and manual responses. Cereb Cortex 2008;18(8):1923–1932. [PubMed: 18245044]

Yarkoni T. Big correlations in little studies: Inflated fMRI correlations reflect low statistical power—commentary on Vul et al. (2009). Perspectives on Psychological Science 2009;4(3):294–298.

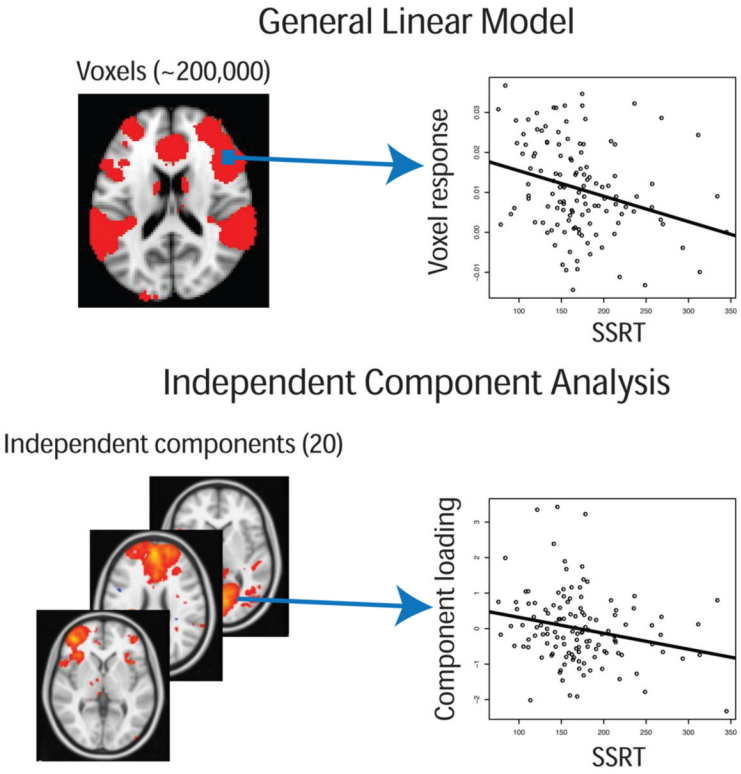

Figure 1. Comparison of Voxelwise vs. ICA Component Correlations with SSRT

(A) Using a whole-brian voxelwise regression approach, activation in individual voxels are correlated with a variable of interest (in this case, SSRT). These correlations are repeated across all voxels in the brain (approximately 200,000) for each person. (B) Using a probabilistic Group ICA approach as applied to activation maps, individual loadings on each component are correlated with a variable of interest (SSRT). These components reflect the subset of voxels that make up a given component and provide a single measure, per person, which can be correlated with the variable of interest (SSRT). Statistical images are overlayed on an average cortical surface. (Right=Right. SSRT, Stop-signal reaction time; ICA, independent components analysis)

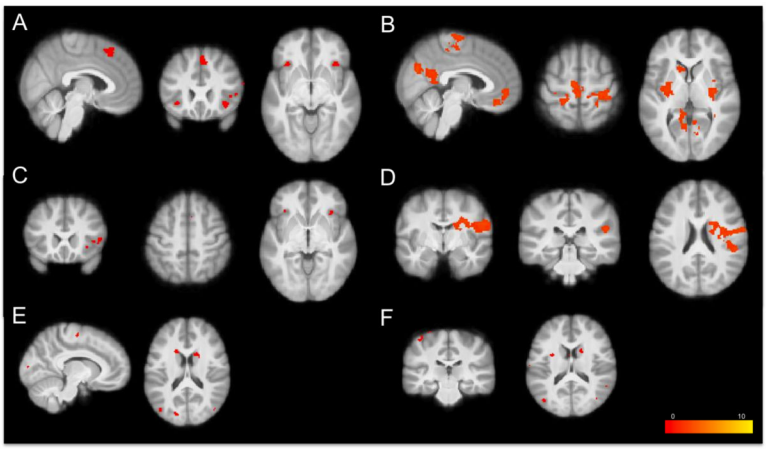

Figure 2. Whole-brain voxel-wise regression analyses of the Stop-signal Task

(A) StopInhibit-Go activation negatively correlated with SSRT ($p < 0.005$ uncorrected) (B) StopInhibit-Go activation positively correlated with SSRT ($p < 0.05$ corrected) (C) StopInhibit-StopRespond activation negatively correlated with SSRT ($p < 0.005$ uncorrected) (D) StopInhibit-StopRespond activation positively correlated with SSRT ($p < 0.05$ corrected) (E) Go-Null activation negatively correlated with median Go RT ($p < 0.005$ uncorrected) (F) Go-Null activation negatively correlated with Go RT standard deviation ($p < 0.005$ uncorrected). Statistical maps were projected onto an average cortical surface using CARET; sagittal, coronal, and axial slices are included to show additional activation with coordinates in MNI space. (Right = Right. SSRT = Stop-signal reaction time)

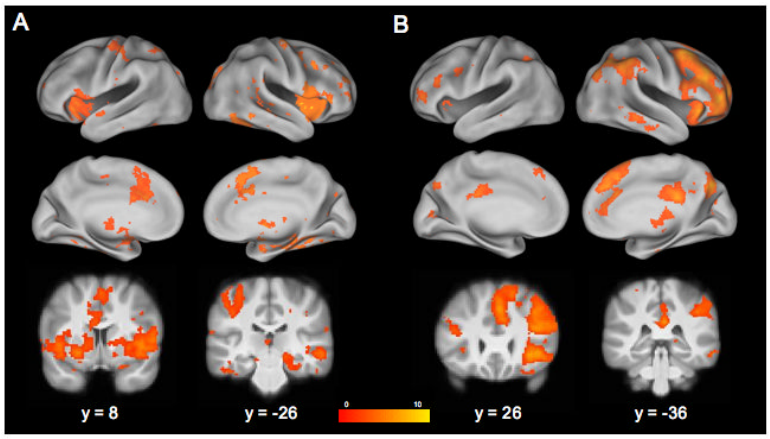

Figure 3. Stopping Components Negatively Correlated with SSRT

StopInhibit-Go ICs from Group ICA analysis of the Stop-signal task that are negatively related with SSRT. (A) IC 14; (B) IC 2. Statistical maps were projected onto an average cortical surface using CARET; coronal slices are included to show additional activation with coordinates in MNI space. (Right=Right.)

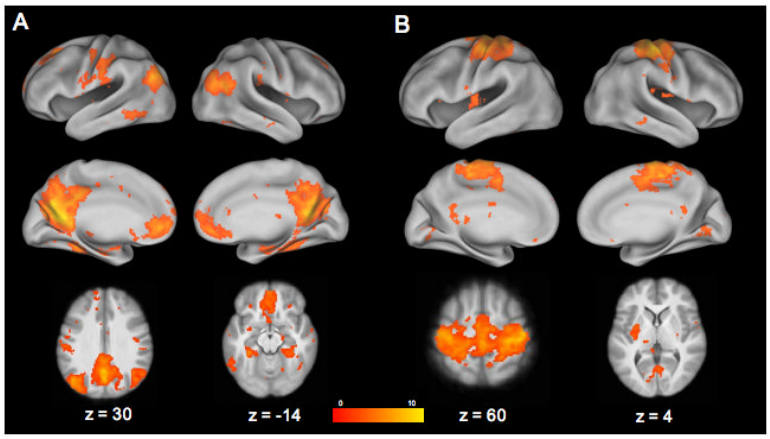

Figure 4. Stopping Components Positively Correlated with SSRT

StopInhibit-Go ICs from Group ICA analysis of the Stop-signal task that are positively related with SSRT. (A) IC 1; (B) IC 9. Statistical maps were projected onto an average cortical surface using CARET; axial slices are included to show additional activation with coordinates in MNI space. (Right = Right.)

Table 1

Descriptive statistics of Stop-signal task performance of all participants included in the present analysis (N = 126).

Variable	Mean	SD	Minimum	Maximum
Age	21.40	4.12	18	39
Median Go RT	468.73	94.99	319.01	790.84
SD Go RT	105.27	30.68	37.10	170.07
Percent Go Responding	98.39	3.12	81.77	100.00
Percent Incorrect Go	1.06	1.42	0.00	7.18
Percent Stop Inhibition	51.38	7.35	28.12	75.00
SSRT	170.64	50.74	75.76	344.86

SD, standard deviation; RT: reaction time; SSRT, stop-signal reaction time.

Neuroimage. Author manuscript; available in PMC 2011 November 1.

Table 2

Clusters of StopInhibit-Go ICs negatively associated with SSRT.

Brain region	Hemisphere	Voxels	z-stat	x	y	z
Clusters of StopInhibit-Go IC 14						
Frontal operculum/insula/orbital cortex/IFG/ precentral gyrus/putamen	R	1987	7.71	48	18	−6
Frontal operculum/insula/orbital cortex/IFG/ precentral gyrus/putamen	L	1642	5.95	−40	14	0
Paracingulate/ACC/SFG	R/L	809	5.06	0	12	52
Occipital fusiform gyrus/lateral occipital cortex	R	411	4.42	40	−62	−14
Postcentral/precentral gyrus	L	374	4.25	−48	−22	62
Middle/superior temporal gyrus	R	176	4.44	60	−26	−8
Parahippocampal gyrus	R	150	4.01	18	−28	−10
Caudate/putamen	R	130	4.06	10	4	10
Clusters of StopInhibit-Go IC 2						
Frontal orbital/insula/operculum/MFG/IFG/ Frontal pole/Precentral gyrus	R	8577	7.05	40	24	−4
SFG/paracingulate/ACC	R/L	2107	6.21	4	36	34
Lateral occipital cortex/angular/supramarginal gyrus/ superior parietal lobule	R	2049	6.84	40	−58	40
Precuneus cortex	R	516	6.56	10	−70	40
Posterior cingulate	R/L	453	5.77	6	−36	26
Occipital fusiform gyrus	L	355	4.67	−16	−80	−24
MFG/IFG	L	170	4.07	−48	32	26
Middle temporal gyrus	R	165	4.23	64	−36	−12
Superior parietal lobule/supramarginal gyrus	L	149	3.77	−30	−52	38
Frontal pole	L	127	4.06	−42	46	4
Thalamus	R	157	3.46	10	−26	10

Voxels: number of activated voxels per cluster (or region within cluster); z-stat: maximum z-statistic for each cluster; x, y, z are MNI coordinates for the peak of each cluster. R = Right, L = Left, MFG = middle frontal gyrus, IFG = inferior frontal gyrus, SFG = superior frontal gyrus, ACC = anterior cingulate cortex.

Table 3

Clusters of StopInhibit-Go ICs positively associated with SSRT.

Brain region	Hemisphere	Voxels	Max z-stat	x	y	z
Clusters of StopInhibit-Go IC 1						
Precuneus/cuneal cortex/posterior cingulate	R/L	5644	9.7	−10	−62	16
Frontal medial cortex/frontal pole/ paracingulate/ACC/subcallosal cortex	R/L	1894	7.77	0	52	−8
Lateral occipital cortex	L	1256	6.93	−32	−78	40
Angular gyrus/lateral occipital cortex	R	1067	5.5	46	−56	20
Superior/middle frontal gyrus	L	687	5.92	−22	24	46
Postcentral gyrus	L	633	4.21	−56	−20	32
Temporal fusiform cortex/parahippocampal gyrus	R	424	4.21	30	−38	−16
Temporal fusiform cortex/parahippocampal gyrus	L	286	5.24	−32	−38	−14
Inferior temporal gyrus/lateral occipital cortex	L	164	3.99	−56	−56	−10
Frontal pole	R	137	4.36	26	38	36
Clusters of StopInhibit-Go IC 9						
Precentral/postcentral gyrus/SMA/SFG/posterior/anterior cingulate/superior parietal lobule/supramarginal gyrus	R/L	11579	9.59	−14	−22	74
Cerebellum/lingual gyrus	R/L	824	4.80	12	−54	−18
Posterior cingulate/precuneus	R/L	265	4.20	2	−52	24
Putamen/insular cortex	L	238	4.16	−30	−2	4

Voxels: number of activated voxels per cluster (or region within cluster); z-stat: maximum z-statistic for each cluster; x, y, z are MNI coordinates for the peak of each cluster. SSRT = Stop-signal reaction time, R = Right, L = Left, ACC = anterior cingulate cortex, SMA = supplementary motor area, SFG = superior frontal gyrus.